Orientational behavior of quantum rotors physisorbed on boron nitride

Kiho Kim and N. S. Sullivan
Department of Physics, University of Florida, Gainesville, Florida 32611-8440
(Received 24 October 1996)

We report the results of NMR studies of the two-dimensional (2D) phase diagrams for molecular H_2 films (monolayers and submonolayers) adsorbed on BN for ortho-H_2 concentrations $0.3<X<0.745$ and temperatures $0.05<T<4.2$ K. A 2D quadrupolar glass state has been identified for submonolayer coverages for $0.48<X<0.69$ and $0.2\leqslant T\leqslant 0.6$ K. For submonolayer films (75% of full monolayer), an orientationally ordered phase (expected pinwheel structure) was observed for $X\geqslant 0.69$ with a transition to a second distinct ordered phase (expected herringbone structure) for $X\leqslant 0.69$. [S0163-1829(97)50702-8]

Studies of the orientational behavior in thin films of quantum rotors (H_2, D_2) are of considerable interest in exploring the effects of reduced dimensions on highly frustrated systems.[1–6] Ortho-H_2 (and para-D_2) molecules with unit angular momentum ($J=1$) represent an almost ideal assembly of interacting ''spin-1'' quantum rotors. At high temperatures, the molecular centers of mass are fixed at the lattice sites but their orientations are thermally disordered. At low temperatures, the highly anisotropic interactions, principally electric quadrupole-quadrupole (EQQ) between $J=1$ molecules and the interactions with the substrate, lead to phase transitions in which the molecular axes are ordered. The behavior in 3D samples is well known[7–11] with a long-range antiferro-orientational Pa_3 configuration[10] at high rotor concentrations and a quadrupolar glass (QG) state[7,8] for $X\leqslant 0.55$.

The interest in these systems is that the intermolecular EQQ interactions are highly frustrated[8,12] due to a fundamental geometrical incompatibility between the symmetry of the interactions and that of the lattice: the lowest energy for a pair of quadrupoles is a ''tee'' configuration with molecular axes mutually perpendicular, but it is impossible to arrange all molecules mutually perpendicular in close-packed lattices. It is the combination of this geometrical frustration and the disorder introduced by the addition of spherical $J=0$ molecules that is believed to result in the QG state. This combination of frustration and disorder is believed to be common to a wide class of glass formers (including magnetic spin glasses), but the underlying physics of the glass formation is not well understood and remains as one of the most outstanding problems of contemporary physics. In view of the geometrical nature of the frustration it is important to determine the influence of restricted geometries on the ordering of frustrated quantum rotors for which the origin of the frustration and the effect of dilution are particularly clear. The knowledge gained from this relatively simple system can provide valuable insight into the behavior of the large family of glass formers.

The purpose of these studies has been to determine the full phase diagram for the orientational ordering of H_2 on a well-defined insulating substrate (BN) for a wide range of ortho concentrations ($0.3<X<0.745$) and temperatures $0.05<T<4.2$ K. We have studied both complete monolayer coverages (incommensurate) and submonolayer coverages (at the expected commensurate $\sqrt{3}\times\sqrt{3}$ density). The orientational ordering for high $J=1$ concentrations ($0.79\leqslant X\leqslant 0.95$) on exfoliated graphite has been determined by the pioneering NMR experiments of Kubik *et al.*[13,14] to be a pinwheel (PW) ordering for $X\simeq 0.9$ for $\sqrt{3}\times\sqrt{3}$ registry (each molecule occupying the center of every third carbon ring) but the full phase diagram for lower X was not explored. The structure determined by Kubik *et al.*[13,14] is consistent with the 2D phase diagram obtained by Harris and Berlinsky[15] from mean-field theory (MFT) that predicted a variety of ordered structures depending on the value of the substrate potential V_c. The MFT ignores fluctuations which are especially significant in 2D, and O'Shea and Klein[16] using Monte Carlo (MC) simulations predicted substantially lower transition temperatures. They used a renormalized EQQ interaction to account for quantum effects. For $V_c=0$, O'Shea and Klein[16] found a PW ordering, and for V_c large enough to force the molecules to lie on a surface they observed a herringbone (HB) structure. A strong V_c tends to align the quantum rotors in the same orientation (standing up or lying down in a plane parallel to the substrate, depending on the sign of V_c) and this competes with the EQQ interactions which favor ''tee'' configurations for each pair. From these simulations, we therefore predict that the ordering would be

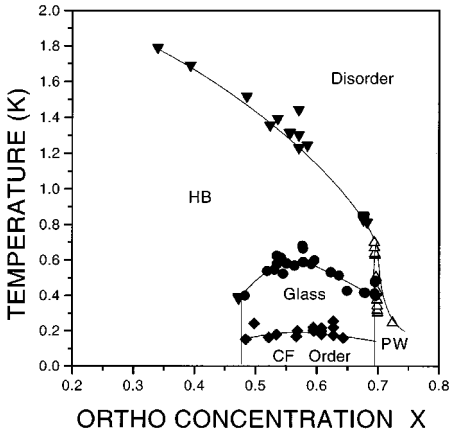

FIG. 1. The phase diagram for a submonolayer (commensurate) film of quantum rotors on BN. The symbols refer to experimental observations of transitions in the line shapes that define the phase boundaries.

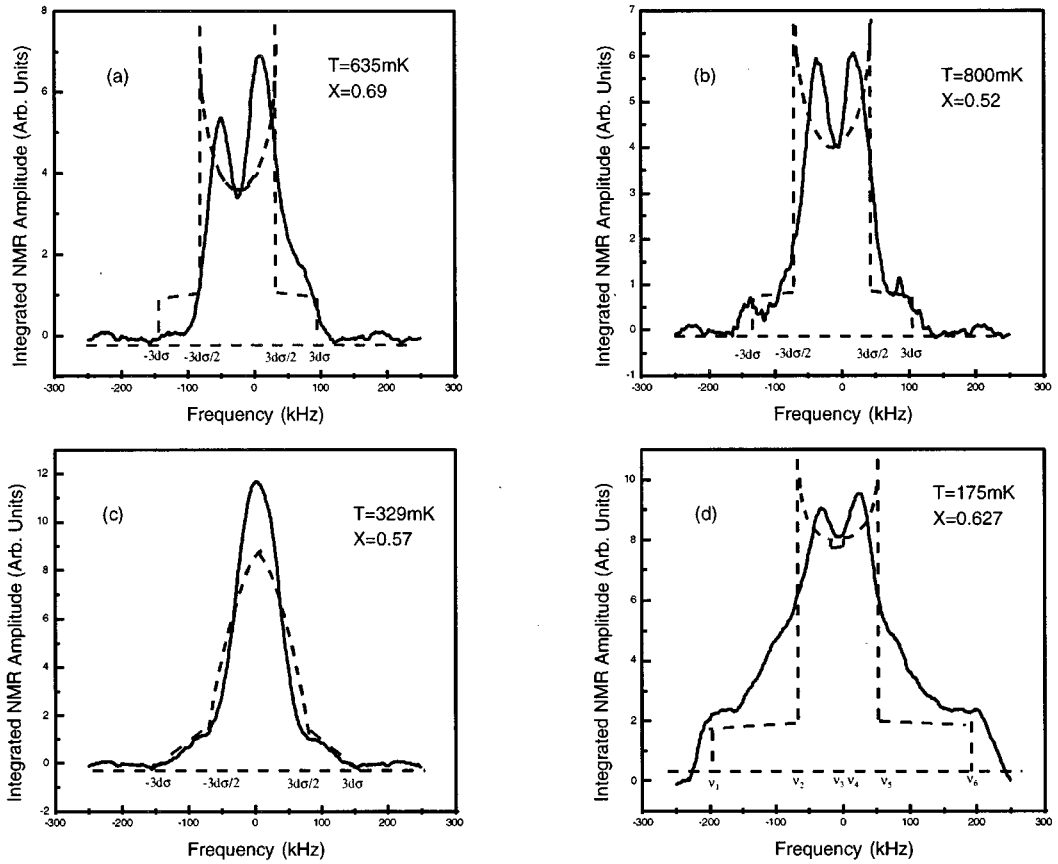

FIG. 2. The submonolayer NMR spectra: (a) pinwheel, (b) herringbone, (c) quadrupolar glass, and (d) CF-ordered. The dotted lines correspond to theoretical models for the different structures. (The dipolar constant $d=57.7$ kHz and the spin-orbit constant $c=113.8$ kHz. $\nu_1=-\nu_6=-c-\frac{15}{4}d\sigma$, $\nu_2=-\nu_5=-\frac{2}{45}c^2/d\sigma-\frac{15}{8}d\sigma$, $\nu_3=-\nu_4=-c+\frac{15}{4}d\sigma$.)

PW for systems dominated by EQQ interactions (i.e., for high X) and that for low X, the ordering would transit to HB. If the disorder is critical for dilute rotor concentrations, a 2D QG state would emerge at low temperatures.

Exfoliated graphite has been extremely well characterized as a substrate and there is a rich variety of phases, commensurate solid (CS) and incommensurate (IS) structures for thin films of physisorbed quantum systems: ^{3}He, ^{4}He, H_2, HD, and D_2.[17–20] Thermal measurements (isotherm studies[1–3] and heat capacity[21–25]) of gases adsorbed on graphite have shown indications of transitions to new ordered structures in 2D. The lattice structures were determined using neutron scattering,[5,26] and low-energy electron diffraction.[18,27,28] This characterization of the lattice structures for H_2 on graphite is particularly important for testing the theoretical models of the orientational ordering. Unfortunately, graphite is not the best substrate for NMR studies because of its anisotropic platelet diamagnetism[29] and the relatively high electrical conductivity at high radio frequencies (RF).[30] These effects distort the NMR line shapes and the phase relationship of the applied RF to the NMR signals[30] so that detailed line shapes are not reliable, particularly in the ultrahigh frequency region. For this reason we have chosen hexagonal BN which is isoelectronic with graphite but has diamagnetic fields that are 40 times smaller.[31] BN has been shown by Shreshta *et al.*,[32] Evans *et al.*,[33] and Crane *et al.*[34] to be a high quality substrate with high homogeneity, large crystallite sizes and relatively low corrugations of the substrate potential. The characterization of the lattice structures of adsorbed systems on BN is not as advanced as for graphite, but recent NMR studies of ^{3}He on BN (Ref. 34) have clearly identified the coverage for the commensurate $\sqrt{3}\times\sqrt{3}$ phase (75% of a complete monolayer), with an incommensurate structure at high coverages. Although there are no specific results for H_2 on BN, it is expected that registry will also occur for 75% of a monolayer for H_2 on BN. The precise monolayer coverage is known from careful adsorption isotherm studies of HD on BN.[35]

We have used commercially available BN samples.[36] The samples must be carefully cleaned and annealed to achieve the highest homogeneity and to remove any impurities associated with the manufacturing process. Following Shreshta *et al.*,[32] we washed the samples in methanol and rinsed the powder with deionized water, being certain to filter and dry the BN powder each time. The sample was outgassed for 4 h at 200 °C and then annealed for 24 h at 900 °C under a vacuum of 10^{-6} Torr. The BN was loaded into a Kel-F NMR sample cell[37] as a loose, uncompressed powder. Thermal contact was assured by inserting a bundle of fine copper wires into the powder with one end of the wires soldered to a copper flange attached to the cold finger of a dilution refrigerator. High-purity normal H_2 gas was physisorbed onto the BN at 20 K using the calibrated volume for completion of a monolayer (IS phase) and 85% of a monolayer for the CS phase. It was necessary to add 10% more than the known

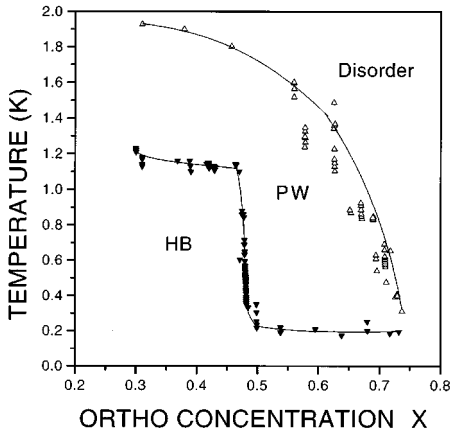

FIG. 3. The phase diagram for a monolayer (incommensurate) film of quantum rotors on BN. The symbols correspond to changes in the NMR line shapes.

exact registry density of 75% to cover the ''lost'' area (~6% dust component, ~2% for crystallite edges, the brush of copper wires embedded in the BN, and the walls of the sample chamber). We believe it is important to slightly overfill (~1%) the registered $\sqrt{3}\times\sqrt{3}$ density rather than leave a small percentage of vacancies in the CS lattice. H_2 molecules surrounding such vacancies will be displaced forward to vacancy center, creating large undesirable local anisotropic crystal fields. After adsorption of H_2, a small quantity of ^{4}He gas was introduced to completely wet all surfaces to improve thermal contact.

The transition from the rotationally disordered to the orientationally ordered phases can be studied directly using NMR techniques because the NMR line shapes are directly related to the orientational order parameters $\sigma=\langle 1-(3/2)J_z^2\rangle$ and $\eta=\langle J_x^2-J_y^2\rangle$. For ($\sigma$ and η)$\neq 0$, the intramolecular dipole-dipole interactions do not average to zero and lead to a fine structure which for powder distributions of the BN crystallites results in Pake doublet spectra for both HB and PW ordering, but with different signatures (peak-peak separation, etc.). In the case of QG ordering, a distinctive ''helmet'' line shape results from which the order parameter distribution can be determined.[7]

NMR studies alone cannot be used to determine the detailed structures for the ordered phases, but we can determine the changes from one phase to another from clear structural changes in the NMR spectra. We have therefore used the results of the MC simulations to label the different phase changes observed by the NMR studies. Based on the MC simulations, we infer that the ordering for high X is PW and that this phase evolves into a HB structure as X decreases. The PW ordering for high X is also consistent with the observations by Kubik *et al.*[14] for very high X ($X\simeq 0.90$).

The NMR absorption spectra were detected using a 270 MHz continuous wave NMR quadrature hybrid tee spectrometer and recorded by sweeping the magnetic field through the resonance with simultaneous ac modulation (1 G) and lock-in detection. The derivative NMR line shapes from the lock-in were integrated using MATHEMATICA[38]. A low rf excitation of -30 dBm was used to avoid saturation effects, but saturation did occur at very low temperatures where the relaxation times become very long.

The observed NMR spectra show clear changes in the detailed line shapes at the transitions from the high-temperature rotationally disordered states to the orientationally ordered structures. The disordered line shape consists of a narrow [~18 kHz full width at half-maximum (FWHM)] Gaussian line shape and this splits into a Pake doublet structure (central peak separation $\simeq$54.6 kHz) for the transition to the HB phase. The QG line shape is a ''helmet'' shape with a central Gaussian (FWHM$\simeq$89 kHz) sitting on top of a broad line with shoulders extending to $\pm$100 kHz. Finally, at very low temperatures we observe another line shape which consists of a central doublet (separation of 65 kHz) with shoulders extending to a maximum of 405 kHz at the lowest T (360 kHz at the phase boundary, $T\simeq 0.15$ K). This very low-temperature structure (with sharp boundaries to the glass phase at $T\simeq 0.19$ K) is unique and has not been reported for bulk or previous 2D studies.[14] It can only be understood in terms of a crystal-field ordered phase (CF) that leads to hindered rotation and a finite spin-orbit contribution. Detailed fits of Fig. 2(d) can be made using modeling of Dubault *et al.*[39] and will be reported in detail elsewhere.

Guided by the results of the MC simulations, the orientationally ordered phase for $0.5<T<2.0$ K and $X<0.67$ (for the $\sqrt{3}\times\sqrt{3}$ structure) is identified as HB. On lowering the temperature these doublet line shapes change to the broad QG line shapes corresponding to a superposition of Pake doublets. Another Pake doublet structure with larger principal peak separation is seen for high $X>0.67$ and low temperatures, and we identify this as a PW phase consistent with the results of Kubik *et al.*[14] The glass regime separates the two long-range-ordered (PW and HB) regions of the phase diagram except for a small region near $X=0.69$. The NMR line shapes for the powder distribution of the substrate crystallites cannot distinguish between the PW and HB phases and it is the results of the MC simulations together with the results of Kubik *et al.*[13,14] that have been used to make this identification.

The phase diagram for the submonolayer film deduced from these clear changes in the line shapes is given in Fig. 1. The individual line shapes corresponding to the distinct regions of the phase diagram are shown in Fig. 2. The evolution from Fig. 2(a) to 2(c) appears to be continuous but limited to a small temperature interval ($\Delta T\leqslant 90$ mK), and the transition from HB to PW near $X\simeq 0.69$ is relatively sharp but at most a weak first-order transition. The PW and HB line shapes are distinguished by not only a different principal peak separation (62.7 and 54.6 kHz, respectively) but also sharper shoulders for the HB structure [Fig. 2(b)]. The QG line shape is the distinctive triangular helmet shape that can only be explained in terms of a broad distribution $P(\sigma)$ of order parameters. We can fit the line shapes by a superposition of Pake doublets to obtain a qualitative measure of $P(\sigma)$ and will report this elsewhere.

In addition to the submonolayer studies we have also explored the phase diagram for a full monolayer coverage which is expected to be an IS lattice from the results of the ^{3}He NMR studies on BN.[34] The phase diagram inferred from the line shapes discussed above is shown in Fig. 3. We find no evidence for QG ordering for a monolayer coverage, and the distinctive CF-ordered line shape was not seen down to the lowest temperatures explored ($\simeq$50 mK, limited by ther-

mal contact to the BN). A PW structure was observed for high temperatures and high X with a weak (possibly) first-order transition to the HB structure at low ortho concentrations.

The transition from the (high T, high X) PW phase to the HB structure can be understood qualitatively in terms of the competition between the EQQ interaction and the substrate crystal field V_c. As X is reduced the strength of the mean field given by $(X\Gamma)$ (where Γ is the EQQ interaction amplitude per ortho pair) is also reduced, and the decreased $X\Gamma/V_c$ ratio leads to HB ordering at low X. This is essentially the same argument as used by Feng *et al.*[40] to explain the differences in the orientational ordering for CO compared to N_2 on graphite. For CO/graphite one observes a sharp PW ordering at high coverages, but at low coverages a broad diffusive transition to HB ordering is observed. This is to be contrasted with N_2/graphite for which sharp (weak first-order) transitions to HB structures are observed for CS films, and increases in coverage lead to uniaxial compression of the HB phase rather than a PW order.[41,42] This difference for N_2 and CO on graphite was attributed to the difference in Γ/V_c which is 1.5 times stronger for CO than that for N_2.

For N_2 and CO on graphite, no clear evidence for QG formation was observed. We believe that this is due to the absence of substitutional disorder in the system which is introduced naturally for H_2 with the replacement of ortho with para molecules. It is the combination of frustration and disorder that is believed to be responsible for the glass phase. The absence of glass formation in our studies for IS monolayer coverages is not understood. It is possible that the compressed structure pushes the critical concentration for glass ordering to very low ortho concentrations and if this falls below the percolation concentration a glass phase may not be realized.

It is interesting to note that there is a qualitative similarity between the phase diagram for CO/graphite[40] and the phase diagrams reported here with PW ordering dominant at high coverages and HB ordering at low coverages. There is a coexistence region with both PW and HB ordering for CO/graphite at intermediate temperatures and coverages similar to the QG region for H_2/BN. The broad diffusive heat capacity peaks seen for both PW and HB transition for CO in this region could be the signature of a glass phase which would not be identified in the heat-capacity studies. It would be useful to carry out NMR studies in this system to measure the order-parameter distributions directly and test for QG behavior.

To conclude, we have mapped out the phase diagrams for the orientational ordering of ortho-para H_2 mixtures in submonolayer and monolayer coverages on BN. The most significant result is the observation of a new 2D QG state for commensurate films. The overall phase diagrams for the long- range orientationally ordered phases are consistent with those predicted from MC simulations. The detailed phase diagrams and the dependence on the lattice geometry of the adsorbed film for glass formation show the strong interplay between geometrical constraints and the symmetry of the interactions that determines the underlying physics of glass formation in frustrated systems.

We gratefully acknowledge many helpful discussions with J. R. Bodart, A. D. Migone, and M. Chan. We also thank T. Crane and B. Cowan for information about ^{3}He registry on BN. This work was supported by National Science Foundation Grant No. DMR-9216785.

[1] W. A. Steele *et al.*, J. Colloid Interface Sci. **28**, 397 (1968).
[2] A. Thomy and X. Duval, J. Chem. Phys. **67,** 1101 (1970).
[3] Y. Larher, J. Chem. Soc. Faraday Trans. **I 70**, 310 (1974).
[4] F. A. Putnam, Jr. and T. Fort, J. Phys. Chem. **79**, 459 (1975).
[5] J. K. Kjems *et al.*, Phys. Rev. B **13**, 1446 (1976).
[6] J. P. McTague *et al.*, Phys. Rev. Lett. **37**, 596 (1976).
[7] N. S. Sullivan *et al.*, Can. J. Phys. **65**, 1463 (1987).
[8] N. S. Sullivan *et al.*, Phys. Rev. B **17**, 5016 (1978).
[9] M. Nielsen *et al.*, J. Phys. (France) Colloq. **38**, C4-10 (1977).
[10] H. M. James and J. C. Raich, Phys. Rev. **162**, 649 (1967).
[11] Isaac F. Silvera, Rev. Mod. Phys. **52**, 393 (1980).
[12] G. Toulouse, Commun. Phys. **2**, 115 (1977).
[13] P. R. Kubik *et al.*, Phys. Rev. Lett. **41**, 257 (1978).
[14] P. R. Kubik *et al.*, Can. J. Phys. **63**, 605 (1985).
[15] A. B. Harris *et al.*, Can. J. Phys. **57**, 1852 (1979).
[16] S. F. O'Shea *et al.*, Chem. Phys. Lett. **66**, 381 (1979).
[17] For a review, see H. Wiechert, Physica B **169**, 144 (1991).
[18] W. Liu and S. C. Fain, Jr., Phys. Rev. B **47**, 15 965 (1993).
[19] J. Nyeki *et al.*, J. Low Temp. Phys. **101**, 279 (1995); P. Mohandus *et al.*, *ibid.* **101**, 481 (1995).
[20] P. S. Ebey *et al.*, J. Low Temp. Phys. **101**, 469 (1995).
[21] M. Bretz *et al.*, Phys. Rev. A **8**, 1529 (1973).
[22] D. M. Butler *et al.*, Phys. Rev. Lett. **35**, 1718 (1975).
[23] H. Freimuth *et al.*, Surf. Sci. **162**, 432 (1985); **178**, 716 (1986).
[24] F. C. Motteler *et al.*, Phys. Rev. B **31**, 346 (1985).
[25] F. A. B. Chaves *et al.*, Surf. Sci. **189/190**, 548 (1987).
[26] H. J. Lauter, in *Phonons 89*, edited by S. Hunklinger, W. Ludwig, and G. Weiss (World-Scientific, Singapore, 1990).
[27] J. J. Lander and J. Morrison, Surf. Sci. **6**, 1 (1967).
[28] J. Cui and S. C. Fain, Jr., Phys. Rev. B **39**, 8628 (1989).
[29] B. P. Cowan and A. J. Kent, Phys. Lett. **106A**, 54 (1984).
[30] M. Rall *et al.*, Cryogenics **34**, 957 (1994).
[31] J. Zupan *et al.*, J. Appl. Phys. **41**, 5337 (1970).
[32] P. Shreshta *et al.*, Langmuir **10**, 3244 (1994).
[33] M. D. Evans *et al.*, J. Low Temp. Phys. **89**, 653 (1992).
[34] T. Crane *et al.*, Physica B **194-196**, 633 (1994).
[35] M. D. Evans *et al.*, J. Low Temp. Phys. **100**, 535 (1995).
[36] Johnson-Matthey, 30 Bond Street, Ward Hill, MA 01835-8099.
[37] Kiho Kim *et al.*, Cryogenics **36**, 311 (1996).
[38] Wolfram Research, Inc., Champaign, IL 61821.
[39] A. Dubault *et al.*, J. Chem. Phys. **61**, 1000 (1974).
[40] Y. P. Feng *et al.*, Phys. Rev. Lett. **71**, 3822 (1993).
[41] R. D. Diehl and S. C. Fain, Jr., Surf. Sci. **125**, 116 (1983).
[42] Q. M. Zhang *et al.*, Phys. Rev. B **32**, 1820 (1985).